



## RESEARCH ARTICLE

**REVISED** Partial catalytic Cys oxidation of human GAPDH to Cys-sulfonic acid. [version 2; peer review: 2 approved]Andrea Lia <sup>1,2</sup>, Adam Dowle <sup>3</sup>, Chris Taylor<sup>3</sup>, Angelo Santino <sup>2</sup>, Pietro Roversi <sup>1</sup><sup>1</sup>Leicester Institute of Chemical and Structural Biology and Department of Molecular and Cell Biology, University of Leicester, Henry Wellcome Building, Lancaster Road, LE1 7HB, UK<sup>2</sup>Institute of Sciences of Food Production, C.N.R. Unit of Lecce, ia Monteroni, Lecce, 73100, Italy<sup>3</sup>Bioscience Technology Facility Department of Biology, University of York, Wentworth Way, York, YO10 5DD, UK**v2** First published: 01 Jun 2020, 5:114  
<https://doi.org/10.12688/wellcomeopenres.15893.1>Latest published: 25 Aug 2020, 5:114  
<https://doi.org/10.12688/wellcomeopenres.15893.2>**Abstract****Background:** n-Glyceraldehyde-3-phosphate dehydrogenase (GAPDH) catalyses the NAD<sup>+</sup>-dependent oxidative phosphorylation of n-glyceraldehyde-3-phosphate to 1,3-diphospho-n-glycerate and its reverse reaction in glycolysis and gluconeogenesis.**Methods:** Four distinct crystal structures of human n-Glyceraldehyde-3-phosphate dehydrogenase (*HsGAPDH*) have been determined from protein purified from the supernatant of HEK293F human epithelial kidney cells.**Results:** X-ray crystallography and mass-spectrometry indicate that the catalytic cysteine of the protein (*HsGAPDH* Cys152) is partially oxidised to cysteine S-sulfonic acid. The average occupancy for the Cys152-S-sulfonic acid modification over the 20 crystallographically independent copies of *HsGAPDH* across three of the crystal forms obtained is 0.31±0.17.**Conclusions:** The modification induces no significant structural changes on the tetrameric enzyme, and only makes aspecific contacts to surface residues in the active site, in keeping with the hypothesis that the oxidising conditions of the secreted mammalian cell expression system result in *HsGAPDH* catalytic cysteine S-sulfonic acid modification and irreversible inactivation of the enzyme.**Keywords**

GAPDH, cysteine S-sulfonic acid, X-ray crystallography, mass-spectrometry, moonlight enzyme

**Open Peer Review****Reviewer Status**

Invited Reviewers

1

2

**version 2**

(revision)

25 Aug 2020

**version 1**

01 Jun 2020



report



report

1. **Vladimir Muronetz**, Lomonosov Moscow State University, Moscow, Russian Federation
2. **Chaaya I. Raje**, National Institute of Pharmaceutical Education and Research, Mohali, India

Any reports and responses or comments on the article can be found at the end of the article.

**Corresponding author:** Pietro Roversi ([pr159@leicester.ac.uk](mailto:pr159@leicester.ac.uk))

**Author roles:** **Lia A:** Data Curation, Formal Analysis, Investigation, Methodology, Project Administration, Validation, Visualization, Writing – Original Draft Preparation, Writing – Review & Editing; **Dowle A:** Data Curation, Formal Analysis, Investigation, Methodology, Software, Validation, Visualization, Writing – Original Draft Preparation, Writing – Review & Editing; **Taylor C:** Data Curation, Formal Analysis, Investigation, Methodology, Software, Validation, Visualization, Writing – Original Draft Preparation, Writing – Review & Editing; **Santino A:** Conceptualization, Funding Acquisition, Resources, Supervision, Writing – Original Draft Preparation, Writing – Review & Editing; **Roversi P:** Conceptualization, Data Curation, Formal Analysis, Funding Acquisition, Investigation, Methodology, Project Administration, Resources, Software, Supervision, Validation, Visualization, Writing – Original Draft Preparation, Writing – Review & Editing

**Competing interests:** No competing interests were disclosed.

**Grant information:** This work was supported by the Wellcome Trust through a LISCB Wellcome Trust ISSF award [204801; P.R.] and a Wellcome Trust Seed Award in Science [214090; P.R.]. A.L. is the recipient of a PhD Studentship from the Agricultural and Forestry Department (DAFNE) of the University of Tuscia (Viterbo, Italy) and funding from the Italian National Research Council (to A.S.). The York Centre of Excellence in Mass Spectrometry was created thanks to a major capital investment through Science City York, supported by Yorkshire Forward with funds from the Northern Way Initiative, and subsequent support from EPSRC grants [EP/K039660/1; EP/M028127/1].

*The funders had no role in study design, data collection and analysis, decision to publish, or preparation of the manuscript.*

**Copyright:** © 2020 Lia A *et al.* This is an open access article distributed under the terms of the [Creative Commons Attribution License](https://creativecommons.org/licenses/by/4.0/), which permits unrestricted use, distribution, and reproduction in any medium, provided the original work is properly cited.

**How to cite this article:** Lia A, Dowle A, Taylor C *et al.* **Partial catalytic Cys oxidation of human GAPDH to Cys-sulfonic acid. [version 2; peer review: 2 approved]** Wellcome Open Research 2020, 5:114 <https://doi.org/10.12688/wellcomeopenres.15893.2>

**First published:** 01 Jun 2020, 5:114 <https://doi.org/10.12688/wellcomeopenres.15893.1>

**REVISED Amendments from Version 1**

- A new version of [Figure 1](#) has been uploaded (file named Slide1.tiff).
- Two new references have been added [63,64](#).
- Small typos have been corrected (the most important one in the Legend to [Figure 1](#)).

Any further responses from the reviewers can be found at the end of the article

**Introduction**

Mammalian HEK293F cells are routinely used in conjunction with secreted protein expression vectors for recombinant protein production<sup>1</sup>. They owe their popularity to ease of handling, robust growth rate, excellent transfectability, high capacity for recombinant protein expression, low-cost media requirements and low levels of secreted contaminants<sup>2</sup>. Of course, in absence of secretion of the desired recombinant protein at hand, contaminants are the only proteins present in recombinant protein expression systems<sup>3,4</sup>. In the course of a research effort aimed at the purification of recombinant *Chaetomium thermophilum* ERAD mannosidase CtHTM1P from the supernatant of HEK293F cells, we purified, crystallised and determined crystal structures of human n-Glyceraldehyde-3-phosphate dehydrogenase (*HsGAPDH*, EC 1.2.1.12)<sup>5</sup>.

GAPDH is essential for glycolysis and gluconeogenesis; it catalyses the NAD<sup>+</sup>-dependent oxidative phosphorylation of n-glyceraldehyde-3-phosphate to 1,3- diphospho-n-glycerate (and its reverse reaction)<sup>6</sup>. The GAPDH-catalysed forward reaction occurs at an important transition point in glycolysis between the enzymatic steps that consume and generate ATP. Several studies indicate that the enzyme has pleiotropic functions independent of its canonical role in glycolysis<sup>7-9</sup>. In addition to the somatic cells *HsGAPDH* isoform, the human genome encodes a testis-specific isoform *HsGAPDHS* (G3PT\_HUMAN (Uniprot O14556)), which is expressed only in the post-meiotic period of spermatogenesis. In multiple mammalian species the sperm isozyme (GAPDHS) shares about 70% amino acid identity with the somatic isozyme, and possesses an additional 72-residues N-terminal extension. The latter enables association of GAPDHS to the sperm flagellum fibrous sheath, so that the enzyme – together with other glycolytic enzymes - provides a localised source of ATP that is essential for sperm motility<sup>10</sup>.

GAPDH was one of the first enzymes to be crystallised<sup>11,12</sup> and one of the first enzymes whose structure was determined by X-ray crystallography<sup>13,14</sup>. A number of studies have reported the GAPDH catalytic Cys carrying oxidised post-translational modifications. In particular, cysteine sulfenic acid (CSX, see [Figure 1A](#)) has been observed in the structure of rabbit muscle GAPDH<sup>15</sup> (of course, by X-ray diffraction alone, this modification may be difficult to distinguish from S-hydroxy-cysteine

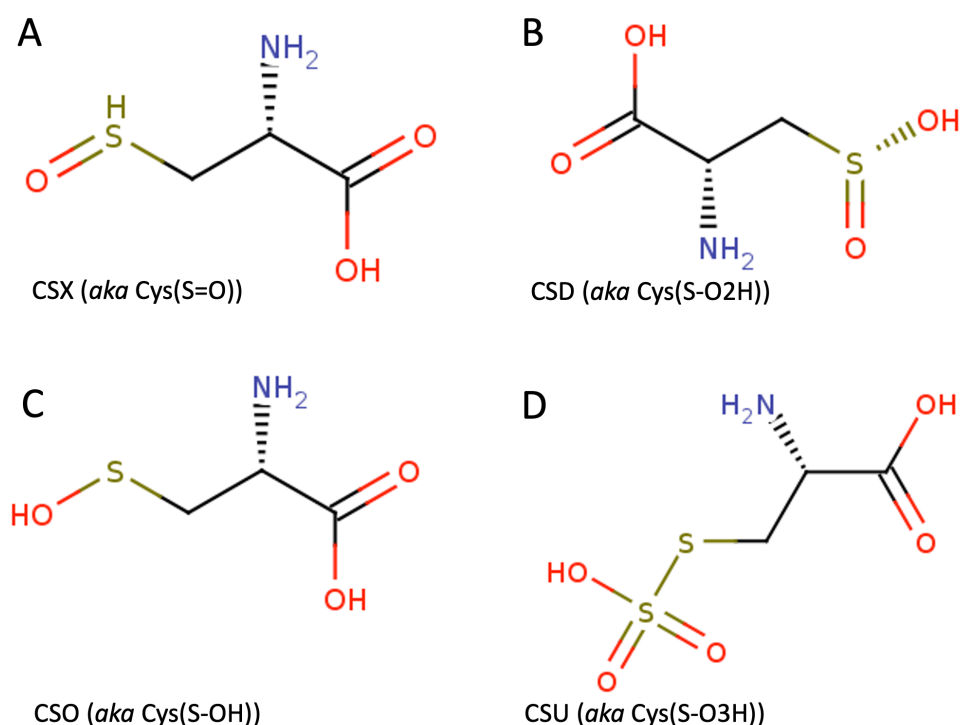


**Figure 1. Cys oxidised modifications and GAPDH PDB entries that carry them at the catalytic Cys152.** **A:** S-Oxy-Cysteine aka Cysteine sulfenic acid (CSX, PDB ID 1J0X); **B:** S-Cysteinesulfinic acid aka S-sulfinocysteine aka 3-Sulfino-L-alanine (CSD, PDB IDs 2VYN and 2VYV); **C:** S-hydroxy-cysteine (CSO, not described in any GAPDH structures); **D:** Cysteine-S-sulfonic acid (CSU, PDB ID 5M6D and this work).

(CSO, see [Figure 1C](#)). Cysteine-S-sulfinic acid (CSD, see [Figure 1B](#)) has been observed in structures of rat GAPDHS and *E. coli* GAPDH<sup>16</sup>. Cysteine-S-sulfonic acid (CSU, see [Figure 1D](#)) modifies the catalytic Cys in a structure of *Streptococcus pneumoniae* GAPDH<sup>17</sup>.

In this paper, we present and discuss mass spectrometry and crystallographic evidence supporting partial oxidation of the catalytic Cys residue of *Hs*GAPDH purified from the supernatant of a HEK293F cell culture. A fraction of the molecules shows Cys-S-sulfonic acid instead of Cys in the active site. The four *Hs*GAPDH crystal structures we describe (which we label as P<sub>2</sub><sub>1</sub> forms A-D, see [Table 1](#)) represent novel *Hs*GAPDH monoclinic polymorphs and are the first *Hs*GAPDH crystal structures carrying a Cysteine-S-sulfonic acid modification of the catalytic cysteine Cys152. Crystal form A is the highest resolution *Hs*GAPDH structure determined to date (1.52 Å).

## Methods

### Cloning

The cloning of the *Chaetomium thermophilum* ERAD mannosidase *Ct*HTM1P (the product of the gene CHTH\_0058730, Uniprot entry [G0SCX7\\_CHATD](#)) in the *Ct*HTM1P<sub>50-1092</sub>-pHLsec vector for secreted mammalian cell expression is described in detail in the Open Laboratory Notebook page (see [Extended data](#)<sup>18</sup>). Briefly, the DNA encoding *Ct*HTM1P<sub>50-1092</sub> was PCR amplified from a commercially obtained plasmid encoding the full length gene, and inserted into the pHLsec vector<sup>2</sup> using ligation independent cloning: the *Ct*HTM1P<sub>50-1092</sub> DNA insert and the *AgeI/KpnI* linearised<sup>AgeI/KpnI</sup> pHLsec DNA were mixed in 3:1 molar ratio: 0.06pmol of *Ct*HTM1P<sub>50-1092</sub> DNA (122 ng) and 0.02pmol of *AgeI/KpnI* linearised pHLsec DNA (60 ng). To this DNA, 10 µL of Gibson Assembly MasterMix(2X) (New England Bioscience E2611L) were added and the total

volume made 20 µL with deionised water. The mix was heated at 50 °C for 1 hour.

### Protein expression

A volume of 450 mL of HEK293F cells at a concentration of 10<sup>6</sup> cells/mL suspended in GIBCO FreeStyle 293 Media (ThermoFisher Scientific 12338018) was transfected with the *Ct*HTM1P<sub>50-1091</sub>-pHLsec vector, using the FreeStyle MAX 293 expression system (Thermo Fisher K900010). Briefly, 1 µg of DNA was used per mL of culture: the DNA vector was initially dissolved in 45 mL of phosphate-buffered saline (PBS: 0.01 M phosphate buffer pH 7.4, 0.0027 M potassium chloride and 0.137 M sodium chloride; PBS tablets, Sigma Aldrich P4417) and vortexed vigorously for 3 seconds; 1.8 mL of a filter-sterilised solution of 0.5 mg/ml polyethylenimine (PEI) was added to the PBS/DNA solution and vortexed vigorously for 3 seconds; the mixture was incubated at room temperature for 20 minutes; the DNA/PEI mixture was added to the cell culture; the cell culture was made 5 µM kifunensine (an inhibitor of endoplasmic reticulum and Golgi mannosidases, Cayman Chemical 109944-15-2). The cell culture was split into three 500 mL Erlenmeyer flasks with 0.2 µm vent caps (Corning), with 150 mL of culture in each flask, and incubated in an orbital shaker incubator at 37°C, shaking at 120 rpm, under a 5% CO<sub>2</sub> atmosphere. The cells' supernatant was harvested 4 days post-transfection by centrifuging at 4,000 x g for 5 minutes.

### Protein purification

The cell supernatant was made 1x PBS by addition of the appropriate volume of 10x PBS stock (obtained by dissolving five PBS tablets (Sigma Aldrich P4417) in 200 mL of deionised water). The pH was adjusted to 7.4 and the solution filter-sterilised through a 0.2 µm bottle-top filter. Nickel immobilised metal affinity chromatography (IMAC) was used as the first step of

**Table 1. Human GAPDH crystal structures.**

Isoform (Uniprot)	PDB ID	Polymorph (Z)	Resolution (Å)	Tetramer PG	Reference
G3P_HUMAN (P04406)	<a href="#">6YND</a>	P2 <sub>1</sub> Form A (16)	1.54	1	This work
	<a href="#">6YNE</a>	P2 <sub>1</sub> Form B (8)	1.85	1	This work
	<a href="#">6YNF</a>	P2 <sub>1</sub> Form C (16)	2.39	1	This work
	<a href="#">6YNH</a>	P2 <sub>1</sub> Form D (8)	2.62	1	This work
	<a href="#">1U8F, 1ZNQ</a>	P2 <sub>1</sub> , 2 <sub>1</sub> , Form A (16)	1.75, 2.50	1	<a href="#">19,20</a>
	<a href="#">3GPD</a>	C2 Form A (8)	3.50	2	<a href="#">21</a>
G3PT_HUMAN (O14556)	<a href="#">4WNC</a>	P2 <sub>1</sub> Form E (16)	1.99	1	<a href="#">22,23</a>
	<a href="#">4WNI</a>	P2 <sub>1</sub> , 2 <sub>1</sub> , Form B (16)	2.30	1	<a href="#">22,23</a>
	<a href="#">6IQ6</a>	P2 <sub>1</sub> Form F (16)	2.29	1	<a href="#">24</a>
	<a href="#">6ADE</a>	I222 (24)	3.15	2 and 222	N/A
	<a href="#">3H9E, 3PFW, 5C7O</a>	C2 Form B (8)	1.72, 2.15, 1.73	2	<a href="#">10,25</a>
	<a href="#">5C7O</a>	P3 <sub>1</sub> , 21 (12)	1.86	2	<a href="#">10</a>

purification. A 5 mL HisTrap HP column (GE Healthcare 17-5248-01) was equilibrated with five column volumes (CV) of binding buffer (50 mM sodium phosphate pH 7.5, 300 mM NaCl, 1 mM TCEP (Sigma Aldrich C4706)). The cell culture supernatant was loaded onto the column at room temperature at a flow rate of 3 mL/min. After a 5CV wash in binding buffer, the column was fitted to an ÄKTA purifier fast protein liquid chromatography (FPLC) machine in a 4°C cabinet and further washed with 6 mL of elution buffer (50 mM sodium phosphate pH 7.5, 500 mM imidazole (Honeywell Fluka 56750), 200 mM NaCl).

The wash fractions from the IMAC run (total volume 4.5 mL) were pooled and concentrated to 2 mL in a polyethersulfone spin concentrator of 10 kDa MW cut-off (Thermo Fisher Scientific 88513). The concentrated sample was filtered through a 0.22  $\mu\text{m}$  spin filter and loaded on a 2 mL loop connected to an ÄKTA purifier FPLC machine in a 4°C cabinet. The sample was injected on a size exclusion chromatography (SEC) S200 16/60 column (GE Healthcare 28-9893-35) equilibrated in filter-sterilised and degassed 20 mM HEPES pH 7.5, 100 mM NaCl and 1mM TCEP (Sigma Aldrich C4706) buffer, and run down the column at 0.4mL/min flow rate, collecting 1 mL elution fractions. *HsGAPDH*-containing fractions were pooled and concentrated as described before to a volume of 70  $\mu\text{L}$ , and protein concentration measured by loading 1.5  $\mu\text{L}$  of sample on a NanoDrop 1000 spectrophotometer (Thermo Scientific). The absorbance was  $\text{OD}_{280}=15.0$ , equivalent to a concentration of 18.8 mg/mL (calculated from  $^{HsGAPDH}\epsilon_{280}=0.7963 \text{ (mg/mL)}^{-1} \text{ cm}^{-1}$ ).

A volume of 30  $\mu\text{L}$  of the *HsGAPDH* obtained from the S200 SEC run was diluted to 500  $\mu\text{L}$  in filter-sterilised and degassed buffer HEPES (Sigma Aldrich H3375) 20 mM pH7.5, NaCl 100 mM, TCEP 1mM and injected onto a Superdex S200 10/300 column equilibrated in the same buffer. The mass of the sample was detected on elution with an 18-angle multi-angle light scattering detector (Dawn® HELEOS® II) coupled with a differential Refractive Index detector (Optilab® T-REX) (Wyatt Technology). Figure 2 illustrates the results of the run. The three fractions C2-C3-C4 eluting between 12.5 and 14 mL were pooled and concentrated to a volume of 45  $\mu\text{L}$  - and a concentration of 3.0 mg/mL.

### Protein crystallisation

Vapour diffusion crystallisation 200 nL sitting drops were set up using a Mosquito crystallisation robot (SPT Labtech), mixing *HsGAPDH* in mother liquor:protein ratios 1:1 (drop 1) and 1:2 (drop 2), with the 96-conditions MORPHEUS crystallisation screen (Molecular Dimensions,<sup>26,27</sup>) and the drops were left equilibrating at 18°C. **P2, Forms A and B:** the protein from the S200 SEC run was set up for crystallisation at a concentration of 18.8 mg/mL. Form A: these crystals grew in drop 2 equilibrated against condition H9 of the MORPHEUS crystallisation screen (Molecular dimensions,<sup>26,27</sup>); 0.1 M Amino acids solution (DL-Glutamic acid, DL-Alanine, Glycine, DL-Lysine, DL-Serine); 0.1 M Buffer System 3 (Tris (base), bicine pH 8.5); 30% v/v Precipitant Mix 1 (40% v/v PEG 500MME, 20% w/v PEG 20000). Form B: these crystals grew in drop 2 equilibrated against condition F9 of the MORPHEUS

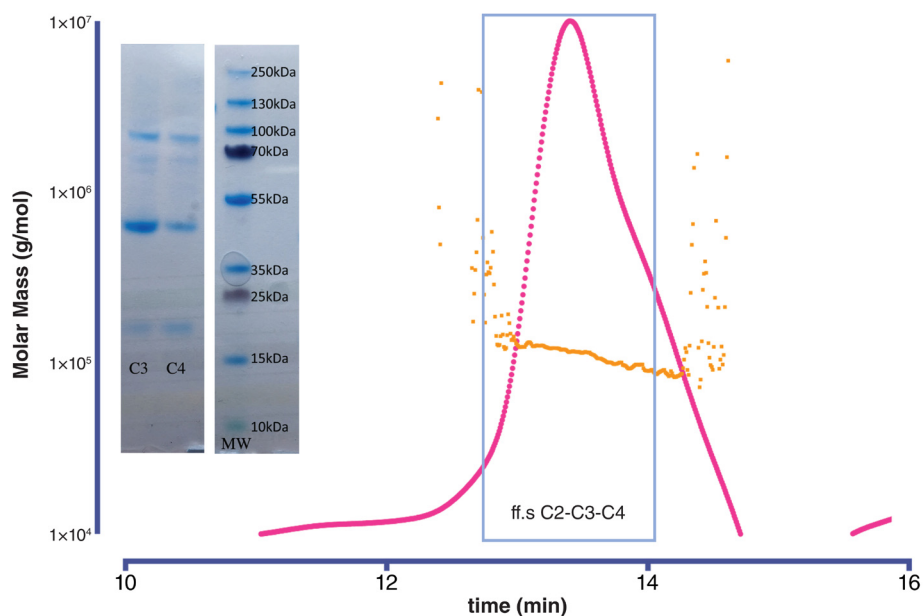


**Figure 2. Size exclusion chromatography multiangle light scattering (SEC-MALS) elution profile of *HsGAPDH*.** Elution profile of the *HsGAPDH* sample run on the SEC S200 10/300 column interfaced with the 18-angle MALS light scattering detector (Dawn HELEOS II®) coupled with a differential refractive index detector (Optilab® T-REX) (Wyatt Technology). The fractions C3-C4 eluting between 13 and 14 mL (boxed) correspond to a *HsGAPDH* tetramer of apparent mass 144 kDa. Inset: the SDS-PAGE NuPAGE Bis-Tris 4-12% gel (Thermo Fisher NP0322PK2), run at 200 V for 30' in MES buffer, stained in Simply Blue™ SafeStain (Thermo Fisher LC6060) for 1 h and destained with water. The unedited gel has been deposited together with the Open Laboratory Notebook page (see *Underlying data*<sup>18</sup>).

crystallisation screen<sup>26,27</sup>: 0.12M monosaccharides solution (D-Glucose, D-Mannose, D-Galactose, L-Fucose, D-Xylose, N-Acetyl-D-Glucosamine); 0.1M Buffer System 3 (Tris (base), bicine pH 8.5) 30% v/v Precipitant Mix 1 (40% v/v PEG 500MME, 20% w/v PEG 20000). **P2<sub>1</sub> Forms C and D**: the protein from the size exclusion chromatography multiangle light scattering (SEC-MALS) run was set up for crystallisation at a concentration of 3.0 mg/mL. Both form C and from D grew in drop 1 equilibrated against the F1 condition of the MORPHEUS crystallisation screen<sup>26,27</sup>: 0.12 M monosaccharides solution (D-Glucose, D-Mannose, D-Galactose, L-Fucose, D-Xylose, N-Acetyl-D-Glucosamine); 0.1 M Buffer System 3 (Tris (base), bicine pH 6.5) 30% v/v Precipitant Mix 1 (40% v/v PEG 500MME, 20% w/v PEG 20000).

### X-ray data diffraction collection and processing

All crystals were cryo-cooled by plunging them into liquid nitrogen. X-ray diffraction data were collected at beamline I03 of the Diamond Light Source in Harwell, England, UK, with an X-ray beam of wavelength  $\lambda=0.97622$  Å and size 80x20  $\mu$ M. Other data collection parameters are listed in Table 2. X-ray diffraction data were processed with the autoPROC suite of programs version 1.0.5<sup>28</sup> with the following command line

```
options: process -h5 Datapath/Data_master.h5 -M HighResCutOnCChalf -d DataOutputDirectory. An alternative Open Source suite that would enable X-ray diffraction data processing in equivalent ways is xia229 running DIALS30.
```

### Structure determination and refinement

**P2<sub>1</sub> Form A**: initial structure factor phases were computed by molecular replacement, searching for eight copies of the *Hs*GAPDH monomer in PDB ID 1U8F in space group P2<sub>1</sub> using the program CCP4-Molrep version 11.7.02<sup>31</sup> with all default parameters. The eight copies of the *Hs*GAPDH monomer are arranged in two tetramers in the asymmetric unit. Initial automated water addition and positional and individual B-factor refinement were carried out in autoBUSTER, version 2.10.3<sup>32,33</sup>. An alternative Open Source piece of software that would enable refinement against X-ray diffraction data in equivalent ways is Vagabond<sup>34</sup>. autoBUSTER was run with the following command line options: refine -m Data.staraniso\_alldata-unique.mtz -p Model.pdb -autoncs -Seq GAPDH.seq -d OutputDir -l XPE.grade\_PDB\_ligand.cif ExcludeBadContacts='EXC LUDE \*|203:\* \*|203:\*' AutomaticFormfactorCorr

**Table 2. Human GAPDH crystal X-ray diffraction data collection parameters and data processing statistics.** Values in parentheses refer to the highest resolution shell.

	Form A	Form B	Form C	Form D
PDB ID	6YND	6YNE	6YNF	6YNH
Det. dist., $d_{max}$ (mm, Å)	198.35, 1.5	288.19, 2.0	253.03, 1.8	356.69, 2.4
Photon flux (photons/s)	$8.84 \times 10^{11}$	$8.88 \times 10^{11}$	$8.85 \times 10^{11}$	$3.88 \times 10^{12}$
Transmission	25%	25%	25%	100%
Number of images	3,600	3,600	3,600	3,600
Oscillation range (°)	0.10	0.10	0.1	0.25
Exposure time (s)	0.05	0.05	0.03	0.013
Space Group	P2 <sub>1</sub>	P2 <sub>1</sub>	P2 <sub>1</sub>	P2 <sub>1</sub>
Cell edges: a,b,c (Å)	81.88, 124.45, 141.99	81.79, 124.65, 79.64	87.14, 111.43, 135.94	87.02, 111.30, 69.74
Cell angle $\beta$ (°)	99.38	117.04	96.02	98.33
Resolution Range (Å)	93.04-1.52 (1.71-1.52)	72.85-1.85 (2.05-1.85)	135.18-2.39 (2.74-2.39)	86.10-2.62 (2.89-2.62)
$R_{merge}$	0.08 (1.07)	0.226 (1.488)	0.27 (1.28)	0.40 (2.47)
$R_{meas}$	0.09 (1.16)	0.245 (1.618)	0.29 (1.38)	0.41 (2.54)
Observations	2,029,459 (100,354)	568,580 (26,433)	418,478 (20,849)	496,488 (24,336)
Unique observations	295,270 (14,763)	81,465 (4,074)	59,243 (2,962)	28,207 (1,409)
Average $I/\sigma(I)$	11.7 (1.7)	6.5 (1.5)	6.5 (1.6)	9.0 (1.5)
Completeness	69.4 (12.2)	67.6 (12.8)	58.2 (8.7)	71.3 (14.0)
Multiplicity	6.9 (6.8)	7.0 (6.5)	7.1 (7.0)	17.6 (17.3)
CC <sub>1/2</sub>	0.997 (0.608)	0.991 (0.456)	0.986 (0.591)	0.990 (0.464)

ection=yes -l CSU.grade\_PDB\_ligand.cif. Automated non-crystallographic restraints were used throughout<sup>35</sup>, including water molecules (assigned to each chain using CCP4-Sortwater version 7.0.078, with all default parameters). At each catalytic Cys152 site, a 0.5:0.5 occupancy ratio mixture of Cys and Cys S-sulfonic acid was initially modelled in unbiased Fo-Fc residual density (see Figure 5). At each Cys152 site, occupancies for Cys and Cys S-sulfonic acid were then refined under the constraint that they sum up to  $1.000 \pm 0.005$ . Crystal form A was deposited in the Protein Data Bank (PDB) with ID code 6YND. Refinement statistics are reported in Table 3. **P2<sub>1</sub> Forms B,C and D:** initial structure factor phases were computed by molecular replacement, searching with the P2<sub>1</sub> Form A tetramer (PDB ID 6YND) in space group P2<sub>1</sub>, placing one tetramer per asymmetric unit in P2<sub>1</sub> Forms B and D and two tetramers per asymmetric unit in P2<sub>1</sub> Form C, using the program CCP4-Molrep<sup>31</sup> version 11.7.02, with all default parameters. The same refinement protocol and restraints were used as described for P2<sub>1</sub> Form A, but with additional external secondary structure restraints<sup>35</sup> to the highest resolution P2<sub>1</sub> Form A structure, using the extra command line flag to `-ref 6YND.pdb` when running autoBUSTER, version 2.10.3<sup>32,33</sup>. An alternative Open Source piece of software that would enable refinement against X-ray diffraction data in equivalent ways is Vagabond<sup>34</sup>. Crystal forms B, C and D were deposited in the PDB with

ID codes 6YNE, 6YNF and 6YNH, respectively. Refinement statistics are reported in Table 3.

### Mass spectrometry

Protein was purified by 1D-PAGE before Coomassie staining and excision for proteomic analysis. Protein was digested in-gel with the addition of 20 ng sequencing grade trypsin (Promega V5111). No reduction or alkylation was performed during digestion to help preserve the native state of oxidation. Resulting peptides were analysed over a 1 h liquid chromatography–mass spectrometry acquisition with elution from a 50 cm EasyNano C18 column as detailed in 36 onto a Thermo Orbitrap Fusion Tribrid mass spectrometer. Spectra were acquired in data dependent acquisition mode with sequential fragmentation of all selected peptide precursors using both higher-energy collisional dissociation and electrontransfer dissociation (ETD). All spectra were acquired in the Orbitrap mass analyser with internal calibration from the ETD reagent.

Product ion spectra were searched against the expected sequence of *Hs*GAPDH (Uniprot P04406) appended to a custom in-house database. All pieces of software were run with default parameters, with the exception that propionamide (+71.037114) and dehydro (-1.007825 Da) were added as manually defined variable modifications. The analysis was carried out using

**Table 3. Human GAPDH crystal structures refinement statistics. Values in parentheses refer to the highest resolution shell, unless otherwise specified.**

	Form A	Form B	Form C	Form D
PDB ID	6YND	6YNE	6YNF	6YNH
Space group (Z)	P2 <sub>1</sub> (16)	P2 <sub>1</sub> (8)	P2 <sub>1</sub> (16)	P2 <sub>1</sub> (8)
Resolution range	140.10-1.52(1.63-1.52)	72.85-1.85 (1.98-1.85)	135.18-2.39 (2.62-2.39)	86.10-2.62 (2.72-2.62)
Reflex.s working set	280,585 (5,242)	77,398 (1,536)	56,303 (1,124)	25,751 (545)
Reflex.s free set	14,686 (332)	4,059 (94)	2,940 (61)	1,459 (20)
R <sub>i</sub> ,R <sub>free</sub>	0.182,0.199 (0.209,0.225)	0.190,0.207 (0.218,0.220)	0.179,0.219 (0.222,0.347)	0.176,0.215 (0.231,0.359)
Rmsd <sub>bonds</sub> (Å)	0.008	0.008	0.009	0.008
Rmsd <sub>angles</sub> (°)	1.02	1.05	1.04	1.03
Ramachandran fav.	97.4% (2,697/2,768)	97.5% (1,304/1,338)	97.0% (2,586/2,667)	97.5% (1,300/1,333)
Ramachandran allow.	99.7% (2,760/2,768)	99.7% (1,334/1,338)	99.5% (2,653/2,667)	99.7% (1,329/1,333)
Tetramers	(A,C,E,H) and (B,D,F,G)	(B,D,F,G)	(A,C,E,H) and (B,D,F,G)	(B,D,F,G)
Occ. Cys-SO <sub>3</sub> H	A:0.13 B:0.15 C:0.09 D:0.18 E:0.13 F:0.15 G:0.15 H:0.08	N/A	A:0.5 B:0.41 C:0.46 D:0.33 E:0.38 F:0.43 G:0.42 H:0.72	B:0.41 D:0.42 F:0.40 G:0.35
Prot.(Wat.) Atoms	20,428 (1,639)	10,108 (569)	20,152 (726)	10,164 (132)
$\langle B \rangle_{prot}$ ( $\langle B \rangle_{wat}$ ) (Å <sup>2</sup> )	27.26 (33.12)	29.40 (36.17)	39.74 (22.93)	45.38 (29.13)

Mascot version 2.6.1 (Matrix Science)<sup>37</sup>, PEAKS Studio X+,10.5 (Bioinformatics Solutions Inc.)<sup>38</sup> and Byonic™ 3.0 (Protein Metrics Inc)<sup>39</sup> search engines (Figure 3A and Figure 4A). The same data analysis was also carried out with freeware, using a combination of MSConvert version 3.0<sup>40</sup>, SearchGui version 3.3.18<sup>41</sup> and PeptideShaker version 1.16.45<sup>42</sup> (Figure 3B and Figure 4B). The resulting peptide assignments are equivalent to the ones obtained with the commercial pieces of software, see Figure 3 and Figure 4. Searching specified a precursor tolerance of 3 ppm and a fragment ion tolerance of 0.02 Da. Initial searches included variable modification of: S-Oxy Cysteine (Figure 1A), Cysteine S-sulphinic acid (Figure 1B), and Cysteine S-sulphonic acid (Figure 1D). Searches were then expanded in PEAKS<sup>38</sup> to include 313 of the most frequently observed proteomic modifications and in Byonic™<sup>39</sup> to include disulfide bonding and wildcard mass addition to Cys.

Peptide spectra matches were filtered to p-values (or equivalents) of <0.05. Individual spectra were manually inspected for site localisation or ambiguity before reporting. Global protein coverage of over 90% was achieved. Individual post-translational modification (PTM) modified spectra were manually inspected for site localisation specificity and potential PTM ambiguity before reporting.

## Results

Since the first crystal structures of the lobster GAPDH enzyme<sup>43–45</sup> several crystal structures of prokaryotic and eukaryotic GAPDHs have been determined. At the time of this writing, the PDB contains more than 142 GAPDH entries, 11 of which are of human GAPDH isoforms (see Table 1). All human GAPDH crystal structures described so far contain tetramers, sitting in crystal sites of three different symmetries: point group 1 (four copies of the monomer all slightly different from each other); point group 2 (dimer of dimers); and point group 222 (four identical copies in a tetramer of exact 222 symmetry).

*Hs*GAPDH crystals of form A and form B grew from the *Hs*GAPDH protein sample purified from the supernatant of HEK293F cells by two chromatography steps (IMAC+SEC); crystals of forms C and form D grew from the same *Hs*GAPDH protein sample after an extra SEC-MALS chromatography step, see Figure 2. Our *Hs*GAPDH crystal structures all contain tetramers of point group 1 (two tetramers per asymmetric unit in forms B and D), and one tetramer per asymmetric unit in forms A and C. Overall, the four novel crystal forms contain 24 crystallographically independent observations of the *Hs*GAPDH molecule, adding to the 29 ones already present in the PDB at the time of this writing (see Table 1). The overall rmsd<sub>Ca</sub> is 0.170 Å

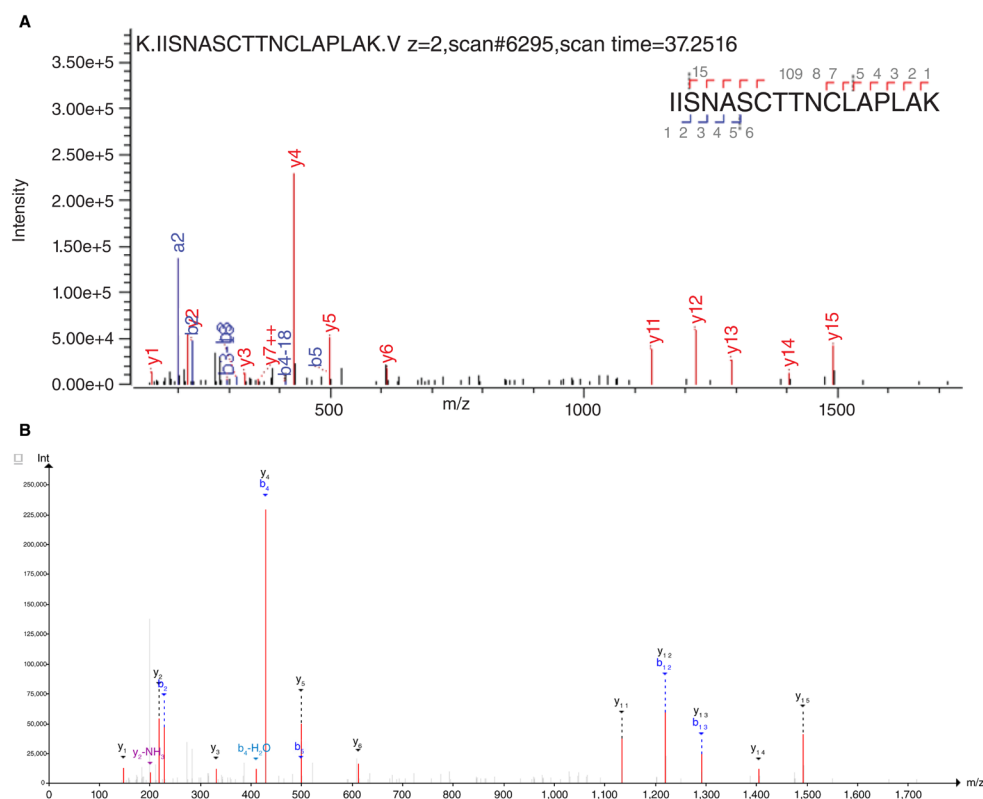


**Figure 3. Product ion spectrum of GAPDH-derived tryptic peptide <sup>146</sup>IISNASCTTNCLAPLAK<sup>162</sup> lacking Cys modification.** Product ions are annotated with theoretical b- and y- ions (fragment ions that appear to extend from the amino- or carboxy-terminus of a peptide, respectively) from the peptide assignment IISNASCTTNCLAPLAK. **A:** data analysed using Mascot<sup>37</sup>, PEAKS<sup>38</sup> and Byonic™<sup>39</sup> search engines, with all default parameters. **B:** data analysed using MSConvert<sup>40</sup>, SearchGui<sup>41</sup> and PeptideShaker<sup>42</sup>.



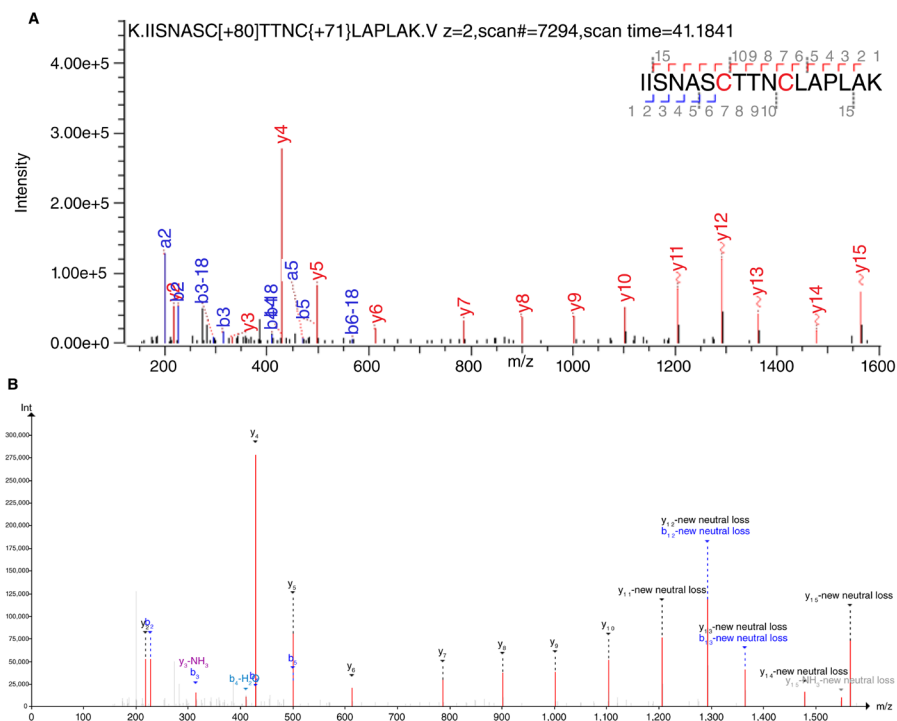


**Figure 4. Product ion spectrum of GAPDH-derived tryptic peptide  $^{146}$ IISNASCTTNC $^{162}$ LAPLAK.** A precursor equating to a mass of 1869.8623 Da was selected and fragmented by HCD. Resulting ions are annotated with theoretical b- and y-ions from the peptide assignment IISNASC(+79.9568 Da)TTNC(+71.036 Da)LAPLAK using the Byonic™ search engine. Annotation of acrylamide adduct modification (+71.036 Da) at Cys156 is implicitly localised from the m/z difference between the product ions y6 and y7. Cys-S-sulfonic acid modification at Cys152 is implied from the difference in mass between the precursor selected and the resulting y11-15 m/z values observed as neutral mass products labelled with “~”. The measured neutral mass difference is 79.9568 Da, equating to a mass error of 0.018 mDa for S-sulfonic acid modification. **A:** data analysed using Mascot<sup>37</sup>, PEAKS<sup>38</sup> and Byonic™<sup>39</sup> search engines, with all default parameters. **B:** data analysed using MSConvert<sup>40</sup>, SearchGui<sup>41</sup> and PeptideShaker<sup>42</sup>.

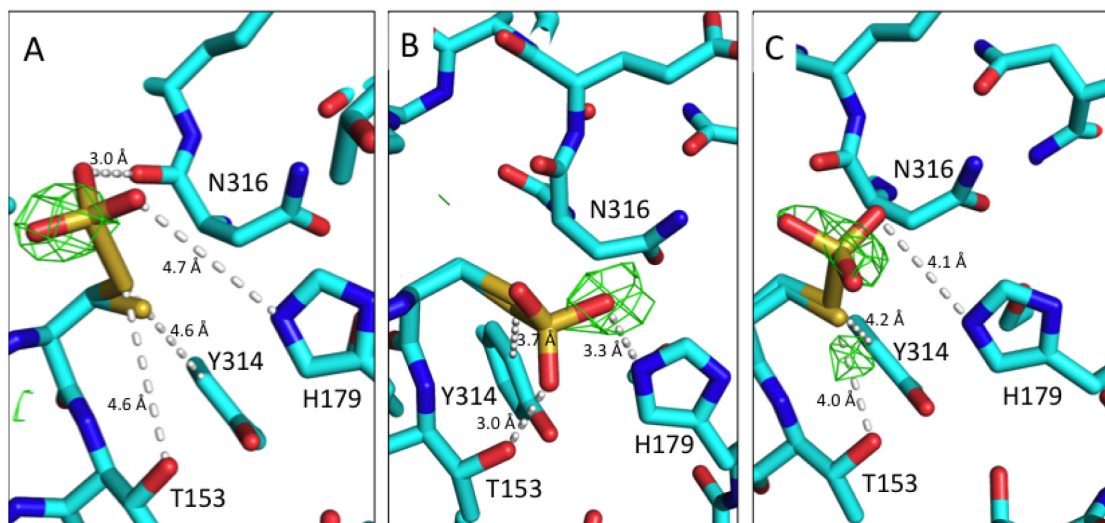


**Figure 5. Fo-Fc difference crystal electron density map around *HsGAPDH* Cys152 residues.** Representative *HsGAPDH* monomers in crystal form C (PDB ID 6YNF) are shown: **A:** monomer B; **B:** monomer E; **C:** monomer G. The 2.5  $\sigma$  contour of the unbiased Fo-Fc map is depicted as a green mesh (the map was calculated with phases from the model before the Cys-S-sulfonic acid modification was built). Residue *HsGAPDH* 152 was modelled and refined as a 0.28:0.72 superposition of Cys:Cys-S-sulfonic acid. C atoms: cyan; N atoms: blue; O atoms: red; S atoms: yellow. Selected non-bonding interactions between the modified Cys and neighbouring residues are represented as white dashed lines with distances in Å. The Figure was made in PyMOL<sup>46</sup>. An alternative Open Source piece of software is UCSF Chimera<sup>47</sup>.

across these 24 crystallographically independent copies of *HsGAPDH*.

The protein sample from which crystal forms C and D were grown was analysed by mass spectrometry. In addition to peptides corresponding to unmodified Cys152 (see Figure 3), we detected ions derived from fragmentation of the Cys152 containing tryptic peptide <sup>146</sup>IISNASCTTNCLAPLAK<sup>162</sup>, which suggests Cys152 S-sulfonic acid modification (Figure 4). Annotation is complicated by the presence of a further modification at Cys156 with a mass addition of +71.036 Da, as directly observed in the fragmentation spectrum by the mass spacing between the y-6 and y-7 ions (Figure 4). The +71.036 Da mass addition at Cys156 is best annotated as acrylamide adduct (propionamide) imparted during PAGE separation<sup>48</sup> rather than being a native modification at this residue. The measured mass of the peptide was 1869.8623 Da and the theoretical mass for the unmodified peptide is 1718.8695 Da. Including the annotated acrylamide adduct, this leaves 79.9568 Da unaccounted for, which is an extremely close match to S-sulfonic acid modification of Cys (+79.9568 Da). A potential ambiguity for the assignment is the similarity in mass of phosphorylation (+79.966331); however, phosphorylation would equate to mass error of 9.5 mDa as opposed to just 0.018 mDa for S-sulfonic acid. Unlike in the case of the acrylamide adduct, the +79.9568 Da mass addition cannot be observed in any of the individual b- or y-ions in the fragmentation spectrum (Figure 4), implying complete neutral loss of the moiety between precursor selection and fragmentation. Although neutral loss is frequently observed with Ser and Thr phosphorylation, it is rarely seen with 100% efficiency, further suggesting sulfation of Cys152 as the most credible assignment. Relative quantification of modified *versus* unmodified peptide forms is not possible based on the mass spectrometry data alone, due to unknown but likely significant differences in relative response resulting from the changes in the physico-chemical properties of the Cys152-containing ions upon Cys-S-sulfation.

Peaks suggesting Cys152 S-sulfonic acid modification are also visible in the initial crystal electron density Fo-Fc difference maps of crystal forms A, C and D<sup>1</sup>, contoured at 2.5 $\sigma$  level or higher, in close proximity to the Cys152  $\gamma$  sulfur atom of most *HsGAPDH* chains in the asymmetric unit (see Figure 5). The orientation of the Cys-S-sulfonic acid moiety in the active site is not unique, but it varies from chain to chain across the three crystal forms. Figure 6A illustrates the modification in the eight copies of *HsGAPDH* in crystal form C. The Cys152 S-sulfonic acid chain makes only loose non-bonding contacts to residues in the active site (see also Figure 5). Modelling of the Cys152 residue as a superposition of Cys and Cys-S-sulfonic acid with variable occupancies in crystal forms A, C and D enables estimation of the extent to which the crystals contain the Cys152 modification. The average occupancy for the Cys152-S-sulfonic

acid modification over these 20 crystallographically independent copies of *HsGAPDH* is 0.31 $\pm$ 0.17 (see Table 3). The *HsGAPDH* monomer with the largest occupancy for the modification (Occ<sub>C<sub>ys-S-SO<sub>3</sub></sub></sub>=0.72) is monomer H in crystal form C. This predominantly Cys-S-sulfonated *HsGAPDH* monomer superposes with an rmsd<sub>C <sub>$\alpha$</sub></sub> =0.423 Å (over 334 C <sub>$\alpha$</sub>  atoms) with the *Streptococcus pneumoniae* GAPDH monomer carrying the same modification<sup>17</sup>, see Figure 6B. When comparing the modified structure to the one of *HsGAPDH* with unmodified Cys152 (PDB ID 1U8F) no significant local changes to active site side chains are observed either (rmsd<sub>C <sub>$\alpha$</sub></sub> =0.127 over 333 C <sub>$\alpha$</sub>  atoms), see Figure 6C. None of the *HsGAPDH* molecules in the crystals contain NAD<sup>+</sup> nor any bound ligand in the active site.

## Discussion and conclusions

GAPDH is mainly a cytoplasmic enzyme, but it has been reported to moonlight as a cell surface and/or extracellular enzyme in healthy human cells<sup>49,50</sup>, in human cells subjected to stresses such as micronutrient starvation, hypoxia, infection, and cancer<sup>50-54</sup>, and to act as an extracellular effector in fungi and bacteria<sup>55-62</sup>. For recent reviews on GAPDH inhibitors and their multiple roles in several pharmacological applications see 63,64.

In our study, *HsGAPDH* was purified from the supernatant of HEK293F cells treated with the mannosidase inhibitors kifunensine and kept for 4 days at 37°C after transfection with a DNA plasmid for recombinant expression of an endoplasmic reticulum glycoprotein. Although kifunensine is toxic to cells only in concentrations higher than the one used (5 $\mu$ M), during the 4 days between transfection and harvesting of the supernatant the experimental conditions are likely harsher than the basal levels of oxidative stress in the HEK293F cell culture media<sup>65</sup>.

Stable oxidation of the GAPDH catalytic cysteine has been observed in a number of studies, for example to Cys sulfenic acid mediated by thiolate oxidation<sup>66</sup>; the modification is reversible but it confers the modified cysteine electrophilic properties similar to the ones of sulfenyl halides<sup>67</sup>. For example, GAPDH catalytic cysteine modification to sulfenic acid converts the enzyme from dehydrogenase to an acyl phosphatase<sup>68-70</sup>. In the presence of excess oxidant, further oxidation of sulfenic acid to sulfinic acid or sulfonic acid is possible. However, in contrast to GAPDH catalytic Cys oxidation to sulfenic acid, which is reversible, oxidation to sulfonic acid leads to irreversible enzyme inactivation and Cys S-sulfonation is generally considered an irreversible form associated with protein misfolding, degradation, and pathology<sup>67</sup>. In particular, S-sulfonated GAPDH has been reported to translocate to subcellular domains where it does not normally occur, where it may stimulate a “gain of function” that could provoke apoptosis<sup>49</sup>.

It is unclear whether the Cys S-sulfonic acid modification we observe in *HsGAPDH* purified from the supernatant of HEK293F cells represents a physiological response of the cells to the recombinant secreted protein expression system conditions, or whether it is simply the outcome of a protracted oxidative environment on the pool of extracellular enzyme instead.

<sup>1</sup> Judging from the crystal electron density difference maps, crystal form B does not seem to have significant Cys152 S-sulfonic acid modification, so in this crystal form residue 152 was modelled as Cys in all chains.

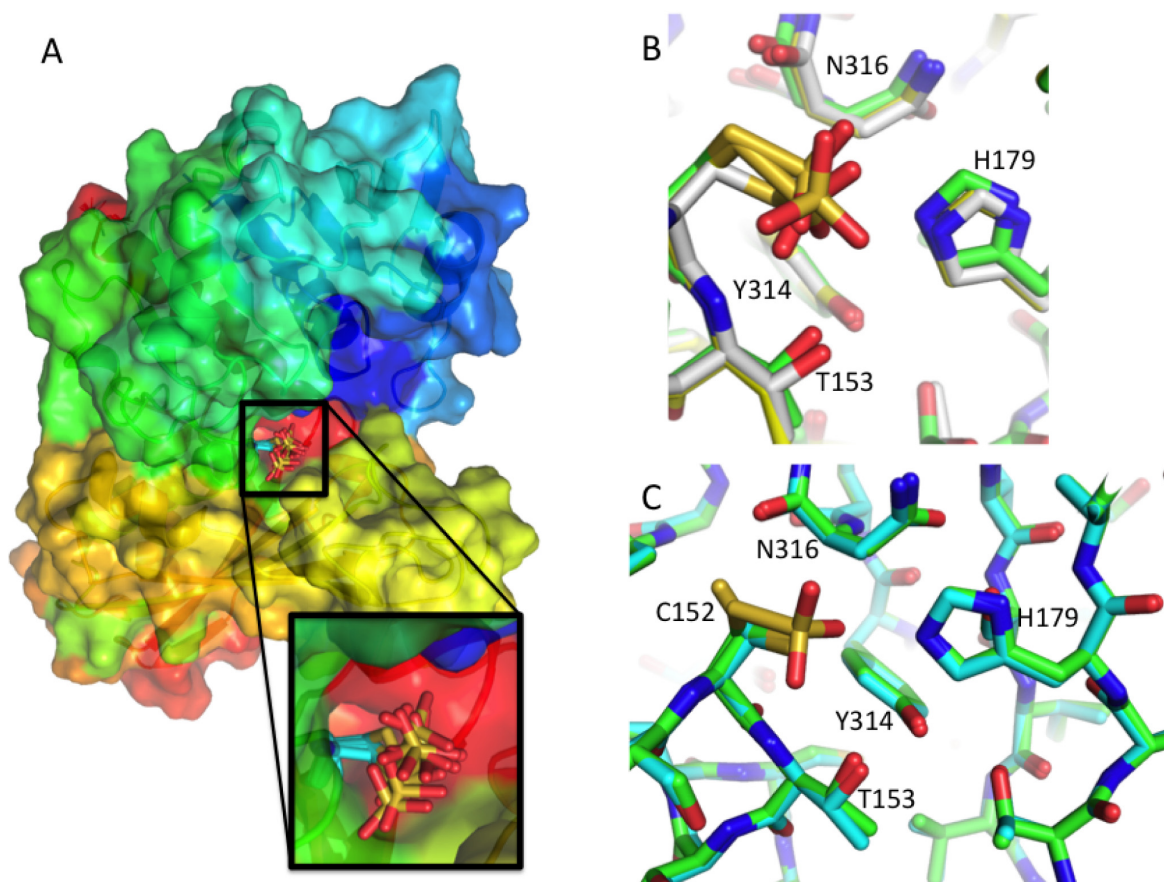


**Figure 6. Cys152-S-sulfonic acid modification of *HsGAPDH*. N atoms: blue; O atoms: red; S atoms: yellow. A:** the Cys152-S-sulfonic acid modification in the 8 copies of *HsGAPDH* in crystal form C. The GAPDH monomer is in surface representation and coloured blue to red from N- to C-terminus. The inset shows the Cys152 S-sulfonic acid chains adopting slightly different conformations in different molecules in the asymmetric unit. **B:** superposition of the active site of Cys152-S-sulfonic acid modified *HsGAPDH* (chain H in crystal form C, green C atoms) with two copies of Cys152-S-sulfonic acid modified *Streptococcus pneumoniae* GAPDH (*SpGAPDH*, PDB ID 5M6D, chain "A", white C atoms; chain "B", yellow C atoms). **C:** superposition of the active site of Cys152-S-sulfonic acid modified *HsGAPDH* (chain H in crystal form C, green C atoms) with native *HsGAPDH* (chain "O" of PDB ID 1U8F, cyan C atoms). The side chain of the catalytic Cys152 of native *HsGAPDH* in PDB ID 1U8F was modelled and refined as a superposition two alternate conformations. The Figure was made in PyMOL<sup>46</sup>. An alternative Open Source piece of software is UCSF Chimera<sup>47</sup>.

GAPDH allostery is mediated by intra-dimer contacts (the active site of one dimer subunit is in close proximity to residues in the neighbouring subunit). The observation that *HsGAPDH* tetramers pack in the crystals in ordered fashion even in presence of partial Cys-S-sulfonic acid modification, together with the overall structural similarity of the Cys S-sulfonated and native monomeric enzymes, suggests that the secreted *HsGAPDH* is constantly inactivated by catalytic Cys S-sulfonation in the expression system's oxidising extracellular environment. Of course, it is also possible that the relative amounts of oxidised vs. reduced GAPDH could vary during protein purification (after harvesting the cells' supernatant) due to changes in the ionic strength and pH; all buffers used were degassed (minimising O<sub>2</sub> content) but contain 1 mM Tris (2-Carboxyethyl) phosphine (TCEP), a reducing agent that prevents intermolecular disulphide\_bond-mediated oligomerisation of GAPDH. The crystallisation conditions do not nominally contain redox active

ingredients but crystal forms A,B grow at pH 8.5, while forms C,D grow at pH 6.5. MS characterisation of GAPDH samples purified at sequential stages during the expression/ purification procedure would elucidate the time-dependence of the enzyme catalytic Cys residue redox composition in the chosen experimental conditions.

#### Data availability

##### Underlying data

X-ray data of forms A, B, C and D at Protein Data Bank, Accession numbers 6YND, 6YNE, 6YNF and 6YNH:

<https://identifiers.org/pdb:6YND>

<https://identifiers.org/pdb:6YNE>

<https://identifiers.org/pdb:6YNF>

<https://identifiers.org/pdb:6YNH>

Mass spectrometry datasets at MassIVE, Accession number MSV000085325: <https://identifiers.org/massive:MSV000085325>

Zenodo: Crystal structure determination of Cys-S-sulfonated HsGAPDH from protein purified from the supernatant of HEK293F cells. <https://doi.org/10.5281/zenodo.3817277><sup>18</sup>

This project contains the following underlying data:

- Gel-Figure3.jpeg (original unedited gel image for Figure 2)

#### Extended data

Zenodo: Crystal structure determination of Cys-S-sulfonated HsGAPDH from protein purified from the supernatant of HEK293F cells. <https://doi.org/10.5281/zenodo.3817277><sup>18</sup>

This project contains the following extended data:

- Copy of the Open Laboratory Notebook (PDF)

- Original unedited gel images for Open Laboratory Notebook (JPG, JPEG and PNG files)

Data are available under the terms of the [Creative Commons Attribution 4.0 International license](https://creativecommons.org/licenses/by/4.0/) (CC-BY 4.0).

#### Acknowledgements

Siyu Wang and Louise Fairall helped with HEK293F cells expression. John W.R. Schwabe gave us access to the SEC-MALS instrument and Christopher J. Millard helped with the SEC-MALLS experiment. Trevor Greenhough coordinates the Midlands Diamond BAG. Neil Paterson helped with the handling of samples at beamline I03 of the Diamond Light Source in Harwell, England, UK. Tony Larson gave us access to resources at the York Centre of Excellence in Mass Spectrometry. Thanks are due to Damir Handzar and Matjaz Hren for their help with retrieval of original un-annotated SDS-PAGE gels from the SciNote backups.

#### References

- Subedi GP, Johnson RW, Moniz HA, *et al.*: **High Yield Expression of Recombinant Human Proteins with the Transient Transfection of HEK293 Cells in Suspension.** *J Vis Exp.* 2015; (106): e53568. [PubMed Abstract](#) | [Publisher Full Text](#) | [Free Full Text](#)
- Aricescu RA, Weixian Lu, Yvonne Jones E: **A time- and cost-efficient system for high-level protein production in mammalian cells.** *Acta Crystallogr D Biol Crystallogr.* 2006; **62**(Pt 10): 1243–1250. [PubMed Abstract](#) | [Publisher Full Text](#)
- Antonyuk SV, Eady RR, Strange RW, *et al.*: **The structure of glyceraldehyde 3-phosphate dehydrogenase from *Alcaligenes xylooxidans* at 1.7 Å resolution.** *Acta Crystallogr D Biol Crystallogr.* 2003; **59**(Pt 5): 835–842. [PubMed Abstract](#) | [Publisher Full Text](#)
- Costanzo LD, Gomez GA, Christianson GW: **Crystal structure of lactaldehyde dehydrogenase from *Escherichia coli* and inferences regarding substrate and cofactor specificity.** *J Mol Biol.* 2007; **366**(2): 481–493. [PubMed Abstract](#) | [Publisher Full Text](#) | [Free Full Text](#)
- Needham DM, Pillai RK: **The coupling of oxido-reductions and dismutations with esterification of phosphate in muscle.** *Biochem J.* 1937; **31**(10): 1837–1851. [PubMed Abstract](#) | [Publisher Full Text](#) | [Free Full Text](#)
- Martin WK, Cerff R: **Physiology, phylogeny, early evolution, and GAPDH.** *Protoplasma.* 2017; **254**(5): 1823–1834. [PubMed Abstract](#) | [Publisher Full Text](#) | [Free Full Text](#)
- Tarze A, Deniaud A, Le Bras M, *et al.*: **GAPDH, a novel regulator of the pro-apoptotic mitochondrial membrane permeabilization.** *Oncogene.* 2007; **26**(18): 2606–2620. [PubMed Abstract](#) | [Publisher Full Text](#)
- Zala D, Hinckelmann MV, Yu H, *et al.*: **Vesicular glycolysis provides on-board energy for fast axonal transport.** *Cell.* 2013; **152**(3): 479–491. [PubMed Abstract](#) | [Publisher Full Text](#)
- Butera G, Mullappilly N, Masetto F, *et al.*: **Regulation of Autophagy by Nuclear GAPDH and Its Aggregates in Cancer and Neurodegenerative Disorders.** *Int J Mol Sci.* 2019; **20**(9): 2062. [PubMed Abstract](#) | [Publisher Full Text](#) | [Free Full Text](#)
- Danshina PV, Qu W, Temple BR, *et al.*: **Structural analyses to identify selective inhibitors of glyceraldehyde 3-phosphate dehydrogenase-S, a sperm-specific glycolytic enzyme.** *Mol Hum Reprod.* 2016; **22**(6): 410–426. [PubMed Abstract](#) | [Publisher Full Text](#) | [Free Full Text](#)
- Warburg O, Christian W: **Isolierung und Kristallisation des Proteins des oxydierenden Gärungsferments.** Springer. 1939.
- Cori GT, Slein MW, Cori CF: **Crystalline d-glyceraldehyde-3-phosphate dehydrogenase from rabbit muscle.** *J Biol Chem.* 1948; **173**(2): 605–618. [PubMed Abstract](#)
- Watson HC, Duée E, Mercer WD: **Low resolution structure of glyceraldehyde 3-phosphate dehydrogenase.** *Nat New Biol.* 1972; **240**(100): 130–133. [PubMed Abstract](#) | [Publisher Full Text](#)
- Rossmann MG, Ford GC, Watson HC, *et al.*: **Molecular symmetry of glyceraldehyde-3-phosphate dehydrogenase.** *J Mol Biol.* 1972; **64**(1): 237–245. [PubMed Abstract](#) | [Publisher Full Text](#)
- Cowan-Jacob SW, Kaufmann M, Anselmo AN, *et al.*: **Structure of rabbit-muscle glyceraldehyde-3-phosphate dehydrogenase.** *Acta Crystallogr D Biol Crystallogr.* 2003; **59**(Pt 12): 2218–2227. [PubMed Abstract](#) | [Publisher Full Text](#)
- Frayne J, Taylor A, Cameron G, *et al.*: **Structure of insoluble rat sperm glyceraldehyde-3-phosphate dehydrogenase (GAPDH) via heterotetramer formation with *Escherichia coli* GAPDH reveals target for contraceptive design.** *J Biol Chem.* 2009; **284**(34): 22703–22712. [PubMed Abstract](#) | [Publisher Full Text](#) | [Free Full Text](#)
- Moreau C, Terrasse R, Thielens NM, *et al.*: **Deciphering Key Residues Involved in the Virulence-promoting Interactions between *Streptococcus pneumoniae* and Human Plasminogen.** *J Biol Chem.* 2017; **292**(6): 2217–2225. [PubMed Abstract](#) | [Publisher Full Text](#) | [Free Full Text](#)
- Roversi P, Lia A: **Crystal structure determination of Cys-S-sulfonated HsGAPDH from protein purified from the supernatant of HEK293F cells.** 2020. <http://www.doi.org/10.5281/zenodo.3817277>
- Jenkins JL, Tanner JJ: **High-resolution structure of human D-glyceraldehyde-3-phosphate dehydrogenase.** *Acta Crystallogr D Biol Crystallogr.* 2006; **62**(Pt 3): 290–301. [PubMed Abstract](#) | [Publisher Full Text](#)
- Ismail SA, Park HW: **Structural analysis of human liver glyceraldehyde-3-phosphate dehydrogenase.** *Acta Crystallogr D Biol Crystallogr.* 2005; **61**(Pt 11): 1508–1513. [PubMed Abstract](#) | [Publisher Full Text](#)
- Mercer WD, Winn SI, Watson HC: **Twinning in crystals of human skeletal muscle D-glyceraldehyde-3-phosphate dehydrogenase.** *J Mol Biol.* 1976; **104**(1): 277–283. [PubMed Abstract](#) | [Publisher Full Text](#)
- White MR, Khan MM, Deredje D, *et al.*: **A dimer interface mutation in glyceraldehyde-3-phosphate dehydrogenase regulates its binding to AU-rich RNA.** *J Biol Chem.* 2015; **290**(3): 1770–1785. [PubMed Abstract](#) | [Publisher Full Text](#) | [Free Full Text](#)
- White MR, Khan MM, Deredje D, *et al.*: **A dimer interface mutation in glyceraldehyde 3-phosphate dehydrogenase regulates its binding to AU-rich RNA.** *J Biol Chem.* 2015; **290**(7): 4129. [Publisher Full Text](#)
- Park JB, Park H, Son J, *et al.*: **Structural Study of Monomethyl Fumarate-Bound**

- Human GAPDH.** *Mol Cells.* 2019; 42(8): 597–603.  
[PubMed Abstract](#) | [Publisher Full Text](#) | [Free Full Text](#)
25. Chaikuad A, Shafqat N, Al-Mokhtar R, et al.: **Structure and kinetic characterization of human sperm-specific glyceraldehyde-3-phosphate dehydrogenase, GAPDS.** *Biochem J.* 2011; 435(2): 401–409.  
[PubMed Abstract](#) | [Publisher Full Text](#)
  26. Gorrec F: **The MORPHEUS protein crystallization screen.** *J Appl Crystallogr.* 2009; 42(Pt 6): 1035–1042.  
[PubMed Abstract](#) | [Publisher Full Text](#) | [Free Full Text](#)
  27. Gorrec F: **The MORPHEUS II protein crystallization screen.** *Acta Crystallogr F Struct Biol Commun.* 2015; 71(Pt 7): 831–837.  
[PubMed Abstract](#) | [Publisher Full Text](#) | [Free Full Text](#)
  28. Vonrhein C, Flensburg C, Keller P, et al.: **Data processing and analysis with the autoPROC toolbox.** *Acta Crystallogr D Biol Crystallogr.* 2011; 67(Pt 4): 293–302.  
[PubMed Abstract](#) | [Publisher Full Text](#) | [Free Full Text](#)
  29. Winter G, Lobley CMC, Prince SM: **Decision making in xia2.** *Acta Crystallogr D Biol Crystallogr.* 2013; 69(Pt 7): 1260–1273.  
[PubMed Abstract](#) | [Publisher Full Text](#) | [Free Full Text](#)
  30. Beilstein-Edmands J, Winter G, Gildea R, et al.: **Scaling diffraction data in the DIALS software package: algorithms and new approaches for multi-crystal scaling.** *Acta Crystallogr D Struct Biol.* 2020; 76(Pt 4): 385–399.  
[PubMed Abstract](#) | [Publisher Full Text](#) | [Free Full Text](#)
  31. Vagin A, Teplyakov A: **Molecular replacement with MOLREP.** *Acta Crystallogr D Biol Crystallogr.* 2010; 66(Pt 1): 22–25.  
[PubMed Abstract](#) | [Publisher Full Text](#)
  32. Blanc E, Roversi P, Vonrhein C, et al.: **Refinement of severely incomplete structures with maximum likelihood in BUSTER-TNT.** *Acta Crystallogr D Biol Crystallogr.* 2004; 60(Pt 12 Pt 1): 2210–2221.  
[PubMed Abstract](#) | [Publisher Full Text](#)
  33. Bricogne G, Blanc E, Brandl M, et al.: **BUSTER 2.10.3.** In BUSTER 2.10.3. 2017.
  34. Ginn HM: **Vagabond: a new project for macromolecular model refinement.** *Acta Crystallographica Section A Crystal Physics, Diffraction, Theoretical and General Crystallography.* 2018; A74: a454.
  35. Smart OS, Womack TO, Flensburg C, et al.: **Exploiting structure similarity in refinement: automated NCS and target-structure restraints in BUSTER.** *Acta Crystallogr D Biol Crystallogr.* 2012; 68(Pt 4): 368–380.  
[PubMed Abstract](#) | [Publisher Full Text](#) | [Free Full Text](#)
  36. de Pablos LM, Ferreira TR, Dowle AA, et al.: **The mRNA-bound Proteome of *Leishmania mexicana*: Novel Genetic Insight into an Ancient Parasite.** *Mol Cell Proteomics.* 2019; 18(7): 1271–1284.  
[PubMed Abstract](#) | [Publisher Full Text](#) | [Free Full Text](#)
  37. Perkins DN, Pappin DJ, Creasy DM, et al.: **Probability-based protein identification by searching sequence databases using mass spectrometry data.** *Electrophoresis.* 1999; 20(18): 3551–3567.  
[PubMed Abstract](#) | [Publisher Full Text](#)
  38. Tran N, Qiao R, Xin L, et al.: **Deep learning enables de novo peptide sequencing from data-independent-acquisition mass spectrometry.** *Nature methods.* 2019; 16(1): 63–66.  
[PubMed Abstract](#) | [Publisher Full Text](#)
  39. Bern M, Kil YJ, Becker C: **Byonic: advanced peptide and protein identification software.** *Curr Protoc Bioinformatics.* Chapter 13:Unit13.20. 2012.  
[PubMed Abstract](#) | [Publisher Full Text](#) | [Free Full Text](#)
  40. Adusumilli R, Mallick P: **Data Conversion with ProteoWizard msConvert.** *Methods Mol Biol.* 2017; 1550: 339–368.  
[PubMed Abstract](#) | [Publisher Full Text](#)
  41. Barsnes H, Vaudel M: **SearchGUI: A Highly Adaptable Common Interface for Proteomics Search and de Novo Engines.** *J Proteome Res.* 2018; 17(7): 2552–2555.  
[PubMed Abstract](#) | [Publisher Full Text](#)
  42. Vaudel M, Burkhardt JM, Zahedi RP, et al.: **Eystein Oveland, Frode S Berven, Albert Sickmann, Lennart Martens, and Harald Barsnes. PeptideShaker enables reanalysis of MS-derived proteomics data sets.** *Nat Biotechnol.* 2015; 33(1): 22–24.  
[PubMed Abstract](#) | [Publisher Full Text](#)
  43. Buehner M, Ford GC, Moras D, et al.: **D-glyceraldehyde-3-phosphate dehydrogenase: three-dimensional structure and evolutionary significance.** *Proc Natl Acad Sci U S A.* 1973; 70(11): 3052–3054.  
[PubMed Abstract](#) | [Publisher Full Text](#) | [Free Full Text](#)
  44. Buehner M, Ford GC, Moras D, et al.: **Structure determination of crystalline lobster D-glyceraldehyde-3-phosphate dehydrogenase.** *J Mol Biol.* 1974; 82(4): 563–585.  
[PubMed Abstract](#) | [Publisher Full Text](#)
  45. Buehner M, Ford GC, Olsen KW, et al.: **Three-dimensional structure of D-glyceraldehyde-3-phosphate dehydrogenase.** *J Mol Biol.* 1974; 90(1): 25–49.  
[PubMed Abstract](#) | [Publisher Full Text](#)
  46. Schrödinger, LLC: **The PyMOL Molecular Graphics System, Version 1.8.0.3.** In: *PyMOL version 1.8.0.3.* 2015.
  47. Pettersen EF, Goddard TD, Huang CC, et al.: **UCSF Chimera-a visualization system for exploratory research and analysis.** *J Comput Chem.* 2004; 25(13): 1605–1612.  
[PubMed Abstract](#) | [Publisher Full Text](#)
  48. Feng CH, Lu CY: **Modification of major plasma proteins by acrylamide and glycidamide: Preliminary screening by nano liquid chromatography with tandem mass spectrometry.** *Analytica chimica acta.* 2011; 684(1–2): 80–86.  
[PubMed Abstract](#) | [Publisher Full Text](#)
  49. Tristan C, Shahani N, Sedlak TW, et al.: **The diverse functions of GAPDH: views from different subcellular compartments.** *Cell Signal.* 2011; 23(2): 317–323.  
[PubMed Abstract](#) | [Publisher Full Text](#) | [Free Full Text](#)
  50. Frederikse PH, Nandanoor A, Kasinathan C: **“Moonlighting” GAPDH Protein Localizes with AMPA Receptor GluA2 and L1 Axonal Cell Adhesion Molecule at Fiber Cell Borders in the Lens.** *Curr Eye Res.* 2016; 41(1): 41–49.  
[PubMed Abstract](#) | [Publisher Full Text](#)
  51. Singh A, Manoj Kumar C, Chaudhary S, et al.: **Moonlighting glycolytic protein glyceraldehyde-3-phosphate dehydrogenase (GAPDH): an evolutionarily conserved plasminogen receptor on mammalian cells.** *FASEB J.* 2017; 31(6): 2638–2648.  
[PubMed Abstract](#) | [Publisher Full Text](#)
  52. Nakano T, Goto S, Takaoka Y, et al.: **A novel moonlight function of glyceraldehyde-3-phosphate dehydrogenase (GAPDH) for immunomodulation.** *Biofactors.* 2018; 44(6): 597–608.  
[PubMed Abstract](#) | [Publisher Full Text](#)
  53. Malhotra H, Kumar M, Singh A, et al.: **Navdeep Sheokand, Chaaya Iyengar Rajee, and Manoj Rajee. Moonlighting Protein Glyceraldehyde-3-Phosphate Dehydrogenase: A Cellular Rapid-Response Molecule for Maintenance of Iron Homeostasis in Hypoxia.** *Cell Physiol Biochem.* 2019; 52(3): 517–531.  
[PubMed Abstract](#) | [Publisher Full Text](#)
  54. Singh Chauhan A, Kumar M, Chaudhary S, et al.: **Trafficking of a multifunctional protein by endosomal microautophagy: linking two independent unconventional secretory pathways.** *FASEB J.* 2019; 33(4): 5626–5640.  
[PubMed Abstract](#) | [Publisher Full Text](#)
  55. Kumar Matta S, Agarwal S, Bhatnagar R: **Surface localized and extracellular Glyceraldehyde-3-phosphate dehydrogenase of *Bacillus anthracis* is a plasminogen binding protein.** *Biochim Biophys Acta.* 2010; 1804(11): 2111–2120.  
[PubMed Abstract](#) | [Publisher Full Text](#)
  56. Muñoz-Provencio D, Pérez-Martínez G, Monedero V: **Identification of Surface Proteins from *Lactobacillus casei* BL23 Able to Bind Fibronectin and Collagen.** *Probiotics and antimicrobial proteins.* 2011; 3(1): 15–20.  
[PubMed Abstract](#) | [Publisher Full Text](#)
  57. Vanden Bergh P, Heller M, Lagache SB, et al.: **The *Aeromonas salmonicida* subsp. *salmonicida* exoproteome: global analysis, moon-lighting proteins and putative antigens for vaccination against furunculosis.** *Proteome Sci.* 2013; 11(1): 44.  
[PubMed Abstract](#) | [Publisher Full Text](#) | [Free Full Text](#)
  58. Nagarajan R, Ponnuraj K: **Cloning, expression, purification, crystallization and preliminary X-ray diffraction analysis of glyceraldehyde-3-phosphate dehydrogenase from *Streptococcus agalactiae* NEM316.** *Acta Crystallogr F Struct Biol Commun.* 2014; 70(Pt 7): 938–941.  
[PubMed Abstract](#) | [Publisher Full Text](#) | [Free Full Text](#)
  59. Martín R, Sánchez B, Urdaci MC, et al.: **Effect of iron on the probiotic properties of the vaginal isolate *Lactobacillus jensenii* CECT 4306.** *Microbiology.* 2015; 161(Pt 4): 708–718.  
[PubMed Abstract](#) | [Publisher Full Text](#)
  60. Borgdorff H, Gautam R, Armstrong SD, et al.: **Cervicovaginal microbiome dysbiosis is associated with proteome changes related to alterations of the cervicovaginal mucosal barrier.** *Mucosal Immunol.* 2016; 9(3): 621–633.  
[PubMed Abstract](#) | [Publisher Full Text](#)
  61. Frohnmeier E, Deptula P, Nyman TA, et al.: **Secretome profiling of *Propionibacterium freudenreichii* reveals highly variable responses even among the closely related strains.** *Microb Biotechnol.* 2018; 11(3): 510–526.  
[PubMed Abstract](#) | [Publisher Full Text](#) | [Free Full Text](#)
  62. Grimmer J, Dumke R: **Organization of multi-binding to host proteins: The glyceraldehyde-3-phosphate dehydrogenase (GAPDH) of *Mycoplasma pneumoniae*.** *Microbiol Res.* 2019; 218: 22–31.  
[PubMed Abstract](#) | [Publisher Full Text](#)
  63. Muronetz VI, Melnikova AK, Barinova KV, et al.: **Inhibitors of Glyceraldehyde 3-Phosphate Dehydrogenase and Unexpected Effects of Its Reduced Activity.** *Biochemistry (Mosc).* 2019; 84(11): 1268–1279.  
[PubMed Abstract](#) | [Publisher Full Text](#)
  64. Lazarev VF, Guzova IV, Margulis BA, et al.: **Glyceraldehyde-3-phosphate Dehydrogenase is a Multifaceted Therapeutic Target.** *Pharmaceutics.* 2020; 12(5): 416.  
[PubMed Abstract](#) | [Publisher Full Text](#) | [Free Full Text](#)
  65. Ugarte N, Ladouce R, Radjei S, et al.: **Proteome alteration in oxidative stress-sensitive methionine sulfoxide reductase-silenced HEK293 cells.** *Free Radic Biol Med.* 2013; 65: 1023–1036.  
[PubMed Abstract](#) | [Publisher Full Text](#)
  66. Wages PA, Lavrich KS, Zhang Z, et al.: **Protein Sulfenylation: A Novel Readout of Environmental Oxidant Stress.** *Chem Res Toxicol.* 2015; 28(12): 2411–2418.  
[PubMed Abstract](#) | [Publisher Full Text](#) | [Free Full Text](#)
  67. Gupta V, Carroll KS: **Sulfenic acid chemistry, detection and cellular lifetime.** *Biochim Biophys Acta.* 2014; 1840(2): 847–875.  
[PubMed Abstract](#) | [Publisher Full Text](#) | [Free Full Text](#)

68. Ehring R, Colowick SP: **The two-step formation and inactivation of acylphosphatase by agents acting on glyceraldehyde phosphate dehydrogenase.** *J Biol Chem.* 1969; **244**(17): 4589–4599.  
[PubMed Abstract](#)
69. Allison WS, Connors MJ: **The activation and inactivation of the acyl phosphatase activity of glyceraldehyde-3-phosphate dehydrogenase.** *Arch Biochem Biophys.* 1970; **136**(2): 383–391.  
[PubMed Abstract](#) | [Publisher Full Text](#)
70. Allison WS, Benitez LV: **An adenosine triphosphate-phosphate exchange catalyzed by a soluble enzyme couple inhibited by uncouplers of oxidative phosphorylation.** *Proc Natl Acad Sci U S A.* 1972; **69**(10): 3004–3008.  
[PubMed Abstract](#) | [Publisher Full Text](#) | [Free Full Text](#)

# Open Peer Review

Current Peer Review Status:  

---

## Version 1

Reviewer Report 11 August 2020

<https://doi.org/10.21956/wellcomeopenres.17433.r39295>

© 2020 Raje C. This is an open access peer review report distributed under the terms of the [Creative Commons Attribution License](#), which permits unrestricted use, distribution, and reproduction in any medium, provided the original work is properly cited.



### Chaaya I. Raje

National Institute of Pharmaceutical Education and Research, Mohali, Punjab, India

The authors Lia A et al., provide X-ray crystallography data to define the Cys-152-S-sulfonic acid modification observed in human GAPDH. Post translational modifications are known to modulate the localization and function of GAPDH. This study provides critical structural information that can be utilized by other research groups investigating the diverse cellular functions of this multifaceted protein. Overall the study is focused with excellent discussion, it be a significant contribution in this field. No additional experiments or changes are suggested.

**Is the work clearly and accurately presented and does it cite the current literature?**

Yes

**Is the study design appropriate and is the work technically sound?**

Yes

**Are sufficient details of methods and analysis provided to allow replication by others?**

Yes

**If applicable, is the statistical analysis and its interpretation appropriate?**

I cannot comment. A qualified statistician is required.

**Are all the source data underlying the results available to ensure full reproducibility?**

Yes

**Are the conclusions drawn adequately supported by the results?**

Yes

**Competing Interests:** No competing interests were disclosed.

**Reviewer Expertise:** Protein multifunctionality, host-pathogen interaction, iron metabolism in

M.tuberculosis

**I confirm that I have read this submission and believe that I have an appropriate level of expertise to confirm that it is of an acceptable scientific standard.**

Reviewer Report 13 July 2020

<https://doi.org/10.21956/wellcomeopenres.17433.r39378>

© 2020 Muronetz V. This is an open access peer review report distributed under the terms of the [Creative Commons Attribution License](#), which permits unrestricted use, distribution, and reproduction in any medium, provided the original work is properly cited.



**Vladimir Muronetz**

Belozerskiy Research Institute of Physicochemical Biology, Lomonosov Moscow State University, Moscow, Russian Federation

The article "Partial catalytic Cys oxidation of human GAPDH" by A. Lia et al. contains new and important information on the structure of the active site of GAPDH with the catalytic Cys152 oxidized to sulfonic acid. It is no less interesting that it was possible to isolate this form of oxidized GAPDH from the conditioned medium of human epithelial kidney cells subjected to stress. The disadvantage of this article is the lack of information on the enzymatic activity of the isolated enzyme, in which only part of the active site cysteines is oxidized. These data could show the degree of irreversible oxidation of the enzyme and confirm the results of crystallographic studies. It should also be noted that the reducing agent was added only on the stage of chromatographic purification of the enzyme. It is possible that the irreversible oxidation of GAPDH could occur not only during cell cultivation, but also during the preparation of the conditioned medium for purification (collecting, dilution, and filtration) as well as during its application on the column.

Other comments:

1. In the title, it would be better to indicate precisely the product of cysteine oxidation.
2. The phrase "GAPDH catalyses the reversible NAD<sup>+</sup>-dependent oxidative phosphorylation of n-glyceraldehyde-3-phosphate to 1,3- diphospho-n-glycerate in both glycolysis and gluconeogenesis" is inaccurate, since during gluconeogenesis the reverse reaction takes place.
3. "In multiple mammalian species the sperm isozyme shares about 70% amino acid identity with the somatic isozyme and plays a role in anchoring GAPDHS to the fibrous sheath in the principal piece of the sperm flagellum". The phrase is incomprehensible. It is unclear, what plays a role in anchoring GAPDHS. You can write that the additional N-terminal fragment of the sperm isoenzyme is necessary for anchoring GAPDHS to the fibrous sheath of the sperm flagellum.
4. The designations of the cysteine derivatives in Fig. 1 could be supplemented with those accepted in enzymology (S-OH, SO<sub>2</sub>H, SO<sub>3</sub>H). The accepted name of the protein is D-



glyceraldehyde-3-phosphate dehydrogenase.

5. The Introduction and Discussion are overloaded with references to old articles, but there is not enough references to later works. For example, there are references to the first works of 1969-1972 years on GAPDH isolation and on acylphosphatase activity of GAPDH.
6. Methods. Cloning and isolation of recombinant mannosidase is excessively detailed in Methods. It should be emphasized that the aim of this work was to isolate GAPDH from the conditioned medium and indicate what is critical for the isolation of this enzyme (for example, the importance of using reducing agents to prevent the oxidation of GAPDH). The authors did not decipher the name of the used reducing agent (TCEP - Tris (2-Carboxyethyl) phosphine), which complicates the understanding of the article.
7. Discussion and conclusion. "However, in contrast to sulfenic acid, higher oxidation states of catalytic Cys residues lead to enzyme inactivation " – an incorrect phrase, since the oxidation of the catalytic cysteine to sulfenic acid also leads to disappearance of the dehydrogenase activity, although reversible

**Is the work clearly and accurately presented and does it cite the current literature?**

Partly

**Is the study design appropriate and is the work technically sound?**

Yes

**Are sufficient details of methods and analysis provided to allow replication by others?**

Yes

**If applicable, is the statistical analysis and its interpretation appropriate?**

Yes

**Are all the source data underlying the results available to ensure full reproducibility?**

Yes

**Are the conclusions drawn adequately supported by the results?**

Yes

**Competing Interests:** No competing interests were disclosed.

**Reviewer Expertise:** Enzymology

**I confirm that I have read this submission and believe that I have an appropriate level of expertise to confirm that it is of an acceptable scientific standard.**

Author Response 13 Aug 2020

**Pietro Roversi**, University of Leicester, Henry Wellcome Building, Lancaster Road, UK

We thank the referee for the attention devoted to our manuscript, for their informed and

thoughtful comments, and for the suggestions. We believe we have addressed all of them and we are confident that the manuscript is improved because of this.

In the following we respond to this Reviewer comments in a point-by-point format.

*The disadvantage of this article is the lack of information on the enzymatic activity of the isolated enzyme, in which only part of the active site cysteines is oxidized. These data could show the degree of irreversible oxidation of the enzyme and confirm the results of crystallographic studies.*

We agree with the Reviewer that enzymatic activity measurements ought to correlate with the percentage of residual reduced catalytic Cys in our sample. Of course, as we state in the discussion, "in contrast to sulfenic acid, higher oxidation states of catalytic Cys residues lead to enzyme inactivation and Cys S-sulfonation is generally considered an irreversible form associated with protein misfolding, degradation, and pathology (Reference [65])", so enzymatic assays of our oxidised GAPDH would likely add to the literature very little that is not known already.

*It should also be noted that the reducing agent was added only on the stage of chromatographic purification of the enzyme. It is possible that the irreversible oxidation of GAPDH could occur not only during cell cultivation, but also during the preparation of the conditioned medium for purification (collecting, dilution, and filtration) as well as during its application on the column.*

This is a very good point and we have added the following paragraph to the discussion: "Of course, it is also possible that the relative amounts of oxidised vs. reduced GAPDH could vary during protein purification (after harvesting the cells' supernatant) due to changes in the ionic strength and pH; all buffers used were degassed (minimising O<sub>2</sub> content) but contain 1 mM Tris (2-Carboxyethyl) phosphine (TCEP), a reducing agent that prevents intermolecular disulphide\_bond-mediated oligomerisation of GAPDH. The crystallisation conditions do not nominally contain redox active ingredients but crystal forms A,B grow at pH 8.5, while forms C,D grow at pH 6.5. MS characterisation of GAPDH samples purified at sequential stages during the expression/ purification procedure would elucidate the time-dependence of the enzyme catalytic Cys residue redox composition in the chosen experimental conditions."

*Other comments:*

*1. In the title, it would be better to indicate precisely the product of cysteine oxidation.*

We have modified the title to: "Partial catalytic Cys oxidation of human GAPDH to sulfonic acid."

*2. The phrase "GAPDH catalyses reversible NAD<sup>+</sup>-dependent oxidative phosphorylation of n-glyceraldehyde-3-phosphate to 1,3- diphospho-n-glycerate in both glycolysis and gluconeogenesis" is inaccurate, since during gluconeogenesis the reverse reaction takes place.*

We have modified the phrase as follows: "GAPDH is essential for glycolysis and gluconeogenesis; it catalyses the NAD<sup>+</sup>-dependent oxidative phosphorylation of n-glyceraldehyde-3-phosphate to 1,3- diphospho-n-glycerate (and its reverse reaction). The GAPDH-catalysed forward reaction occurs at an important transition point in glycolysis between the

*enzymatic steps that consume and generate ATP."*

3. *"In multiple mammalian species the sperm isozyme shares about 70% amino acid identity with the somatic isozyme and plays a role in anchoring GAPDHS to the fibrous sheath in the principal piece of the sperm flagellum". The phrase is incomprehensible. It is unclear, what plays a role in anchoring GAPDHS. You can write that the additional N-terminal fragment of the sperm isoenzyme is necessary for anchoring GAPDHS to the fibrous sheath of the sperm flagellum. We have modified this sentence along the Reviewer's suggestion: "In multiple mammalian species the sperm isozyme (GAPDHS) shares about 70% amino acid identity with the somatic isozyme, and possesses an additional 72-residues N-terminal extension. The latter enables association of GAPDHS to the sperm flagellum fibrous sheath, so that the enzyme – together with other glycolytic enzymes - provides a localised source of ATP that is essential for sperm motility."*

4. *The designations of the cysteine derivatives in Fig. 1 could be supplemented with those accepted in enzymology (S-OH, SO<sub>2</sub>H, SO<sub>3</sub>H). The accepted name of the protein is D-glyceraldehyde-3-phosphate dehydrogenase.*

We have modified the Figure – adding the conventional names for the Cys derivatives. We include the accepted name of the protein in the first paragraph of the paper.

5. *The Introduction and Discussion are overloaded with references to old articles, but there is not enough references to later works. For example, there are references to the first works of 1969-1972 years on GAPDH isolation and on acylphosphatase activity of GAPDH.*

We include references to early work to give credit to the scientists who first characterised the enzyme. We take the point that it is important to reference more recent work too. We have now included references to two reviews on GAPDH inhibition in order to link to more recent GAPDH work: *"For recent reviews on GAPDH inhibitors and their multiple roles in several pharmacological applications see <sup>69,70</sup>". Ref. 69: Muronetz VI, Melnikova AK, Barinova KV, Schmalhausen EV. Inhibitors of Glyceraldehyde 3-Phosphate Dehydrogenase and Unexpected Effects of Its Reduced Activity. Biochemistry (Mosc). 2019;84(11):1268-1279. doi:10.1134/S0006297919110051; Ref. 70: Lazarev VF, Guzhova IV, Margulis BA. Glyceraldehyde-3-phosphate Dehydrogenase is a Multifaceted Therapeutic Target. Pharmaceutics. 2020;12(5):416. Published 2020 May 2. doi:10.3390/pharmaceutics12050416.*

6. *Methods. Cloning and isolation of recombinant mannosidase is excessively detailed in Methods. It should be emphasized that the aim of this work was to isolate GAPDH from the conditioned medium and indicate what is critical for the isolation of this enzyme (for example, the importance of using reducing agents to prevent the oxidation of GAPDH). The authors did not decipher the name of the used reducing agent (TCEP - Tris (2-Carboxyethyl) phosphine), which complicates the understanding of the article.*

The details on the cloning of the recombinant mannosidase are necessary for full reproducibility of the experiment as it was carried out. We have added the full chemical name of TCEP in the place in the text where it first appears and explained the intended reason for its presence in our protein chemistry buffers: *"all buffers (...) contain 1 mM Tris (2-Carboxyethyl) phosphine (TCEP), a reducing agent that prevents intermolecular disulphide\_bond-mediated oligomerisation of GAPDH.*

7. Discussion and conclusion. *“However, in contrast to sulfenic acid, higher oxidation states of catalytic Cys residues lead to enzyme inactivation” – an incorrect phrase, since the oxidation of the catalytic cysteine to sulfenic acid also leads to disappearance of the dehydrogenase activity, although reversible.*

We have modified the sentence as follows: *“However, in contrast to GAPDH catalytic Cys oxidation to sulfenic acid, which is reversible, oxidation to sulfonic acid leads to irreversible enzyme inactivation”*

**Competing Interests:** We have no competing interests to disclose.

---